

Hypoxia and reoxygenation of primary human hepatocytes induce proteome changes of glucose metabolism, oxidative protection and peroxisomal function

CHRISTOPH W. STREY¹, JOHANNES GESTRICH¹, TOBIAS BECKHAUS², ROSA MARIA MARQUEZ-PINILLA¹, ELSIE OPPERMAN¹, CHRISTIAN MÖNCH¹, JOHN D. LAMBRIS³, MICHAEL KARAS² and WOLF O. BECHSTEIN¹

¹Department of General and Vascular Surgery, Johann Wolfgang Goethe-University Frankfurt, Medical School, Frankfurt;

²Institute of Pharmaceutical Chemistry, Johann Wolfgang Goethe University Frankfurt, Frankfurt, Germany; ³Department of Pathology and Laboratory Medicine, University of Pennsylvania, School of Medicine, Philadelphia, PA 19104, USA

Received April 19, 2010; Accepted June 14, 2010

DOI: 10.3892/ijmm_00000502

Abstract. Protective hepatocellular responses to a hypoxic challenge are crucial to preserve liver function. The knowledge of affected metabolic functions could help assess and enhance hepatic ischemic tolerance. Here we studied adaptive mechanisms in human hepatocytes after hypoxia and reoxygenation using a proteomic approach. Proteins from primary hepatocytes were extracted after 6 h of hypoxia and 24 h of reoxygenation. The proteome was analyzed by 2D-electrophoresis. Densitometry and mass spectrometry (MALDI-TOF-MS) were used for protein identification. Two hundred and sixty-two spots were differentially analyzed and 33 spots displayed significant differences between hypoxic and normoxic cells. Seventeen proteins were identified by mass spectrometry. After hypoxia and reoxygenation the UTP-glucose-1-phosphate uridyltransferase, phosphoglycerate kinase1, fructose-1,6-bisphosphate aldolase, glyceraldehyde-3-phosphate dehydrogenase, fructose-1,6-bisphosphatase, thiosulfat-sulfurtransferase, thioredoxin peroxidase, peroxi-redoxin III, and annexin A2 proteins were down-regulated. An increased expression was found for carbamoyl phosphate synthetase I, heat shock 70 kDa protein5, phosphoenol-pyruvate carboxy-kinase, catalase isoform2, peroxiredoxin II, glutathione S-transferase, hydroxyacid oxidase1, and F1-ATP synthase, α subunit1. Hepatocellular adaptation to hypoxia and reoxygenation involve glucose metabolism, peroxisomal functions, and oxidative stress protection. The identified proteins can serve as possible diagnostic targets to monitor

hepatic hypoxic tolerance e.g. in the context of liver surgery and transplantation.

Introduction

Hepatic ischemia/reperfusion-induced injury (IRI) is a concern in various clinical settings, including liver transplantation (LTX) and general liver surgery. Cold preservation of liver grafts is associated with prolonged ischemia and followed by reoxygenation during the reperfusion phase. The process of IRI initiates many pathophysiological mechanisms with damaging consequences for the liver graft. The length of cold ischemia time is a determinant for the degree of graft damage during the early and late phase of reoxygenation. Furthermore, other clinical factors such as donor age, lipid and energy status as well as fatty degeneration of the organ contribute to the magnitude of cold storage and reperfusion insult. All these factors may lead to early and late liver graft dysfunction. The adaptive mechanisms that are initiated due to IRI also at the cellular level of the hepatocytes, which enable the liver graft to regain function are still not well defined.

A proteomic study of the process of hypoxia and reoxygenation (HR) in primary hepatocyte cultures in comparison with hepatocytes under normoxia (N) has not been undertaken yet. The global approach to changes of the proteome could contribute to the understanding of the adaptive mechanisms initiated under HR on a cellular level. Proteomics is a powerful methodology that allows assessment of global alterations in biological systems at the protein level (1,2). Proteomic techniques have been employed to investigate the *in vivo* and *in vitro* proteome response of cells and animal models to drugs, diseases and trauma (3-6).

By using comparative proteome analysis via two-dimensional gel electrophoresis (2-DE) between hepatocytes cultured under normoxic conditions and hepatocytes undergoing a sequence of prolonged HR, differentially expressed proteins can be identified by matrix-assisted laser-desorption ionization-time-of-flight mass spectrometry (MALDI-TOF-

Correspondence to: Dr Christoph W. Strey, Department of General and Vascular Surgery, Johann Wolfgang Goethe-University Frankfurt, Theodor-Stern-Kai 7, 60590 Frankfurt am Main, Germany
E-mail: strey@gmx.de

Key words: human hepatocytes, hypoxia/reoxygenation, cell culture, mass spectrometry, two dimensional gel electrophoresis

MS) and database searching. This approach enabled us to show that a sequence of HR induced protein expression changes in three major functional protein groups in hepatocytes. Among these were proteins from the context of glucose metabolism, oxidative and cellular stress protection and peroxisomal function. The identified cellular functions represent relevant targets for the adaptation processes under the influence of HR.

Materials and methods

Isolation of primary hepatocytes and cell culture. Normal human liver tissue was obtained from liver resection. Informed consent was obtained from each patient included in the study and the study protocol conforms to the ethical guidelines of the 1975 Declaration of Helsinki as reflected in a priori approval by the institution's human research committee. Human hepatocytes were isolated by a two-step collagenase perfusion technique as described before (7). Briefly, a wedge from the resected liver lobe was cut distant from the malignant lesion. Normal liver tissue was perfused (Masterflex pump, Novodirekt, Kehl am Main, Germany) at 37°C with HBSS without $\text{Ca}^{2+}/\text{Mg}^{2+}$ containing 100 $\mu\text{g}/\text{ml}$ gentamycin sulfate and 20 mM HEPES, followed by a perfusion with 0.5 mM EGTA in HBSS without $\text{Ca}^{2+}/\text{Mg}^{2+}$ under recirculation for 15–25 min. Subsequently, the liver tissue was perfused with 0.075% collagenase IV (Sigma) and 5 mM CaCl_2 in HBSS for 10–30 min. Liver cells were gently dispersed in cold HBSS with 20 mM HEPES-buffer and 100 $\mu\text{g}/\text{ml}$ gentamycin sulfate. Hepatocytes were purified by triple centrifugation in DMEM/Ham's F12 medium (5 min, 28 x g). Cell vitality was estimated with trypan dye exclusion and only cells with a vitality >80% were utilized. Hepatocytes were seeded at a density of 1.8×10^5 viable cells per cm^2 onto a collagen I-coated 6-well plate (Biocoat® BD Falcon, Heidelberg, Germany) in DMEM/Ham's medium containing 5% human serum, 10 ng/ml EGF, 100 $\mu\text{g}/\text{ml}$ gentamycin sulfate, 20 mM HEPES.

Cell culture hypoxia and reoxygenation pattern. Four independent experiments with hepatocytes from different donors were performed. Hypoxia was induced by pregassing incubation medium with 100% N_2 for 30 min. Hepatocytes were then incubated in pregassed culture medium and sustained with 100% N_2 for 6 h at 37.0°C and reoxygenated for 24 h. Cells were dislodged using accutase (PAA, Cölbe, Germany), centrifuged at 300 x g for 10 min. Cell pellets were snap-frozen in liquid nitrogen and stored at -80°C.

LDH cytotoxicity assay. Cytotoxic cell death can be evaluated by quantification of plasma membrane leakage of LDH (8). Hepatocyte supernatant was collected and centrifuged at 170 x g for 10 min. Supernatant (100 μl) was transferred into a 96-well microtiter plate and 100 μl of reaction mixture (Cytotoxicity Detection Kit, Roche Diagnostics, Germany) was added and incubated for 30 min. The absorbance was read at 490 nm (Ceres UV 900C, Biotek Instruments Inc., VT, USA).

Oxygen measurements. Oxygen concentration was measured in the culture medium at the beginning and at the end of each experiment (under N_2 atmosphere or under normoxic culture conditions). Oxygen content of the medium was reduced from

150 to 13.5 mmHg as measured by a portable O_2 analyzer (OxyScan graphic, UMS, Meiningen, Germany) according to the manufacturer's instructions.

Two dimensional gel electrophoresis. The 2-DE was performed with Zoom® IPGRunner™ (Invitrogen, CA, USA). In summary, 12×10^6 hepatocytes were lysed in Zoom 2D protein solubilizer. Protein content was determined using Coomassie (Pierce, IL, USA). Zoom® strips pH 3–10 (Invitrogen) were rehydrated in 155 μl rehydrating buffer (8 M Urea; 2% CHAPS; 0.5% Carrier Ampholytes) and pooled protein samples (20 μg each). Pooled protein samples were composed by adding equal protein amounts from cell cultures of four independent cell-isolation and hypoxia experiments. The strips were subjected to isoelectric focusing according to manufacturer's instructions. For the 2nd dimension, NuPAGE® Novex 4–12% bis-tris gels (Invitrogen) were used. 2-DE runs were repeated three times for each pooled sample. Gels were stained with Sypro® Ruby stain (Molecular Probes, Leiden, The Netherlands) according to manufacturer's instructions. Proteins were detected using a Typhoon laser scanner (GE Healthcare, Munich, Germany). The quantification and comparisons of spot abundance was done after gel scanning as described before (3). Digital images were processed using the image software Phoretix 2D (Nonlinear Dynamics, Amersham Biosciences). Protein levels were compared among gels after normalization (total spot intensity). For the determination of significance ($p < 0.05$) the Mann-Whitney test was applied.

Silver staining and spot excision. Before manual spot picking, gels were stained with Silver Stain Plus (Bio-Rad laboratories, CA, USA) according to manufacturer's instructions. Protein spots of interest were excised and stored at -80°C.

Western blot analysis. Hepatocyte lysates (20 μg) were separated on a 7, 10 or 12% SDS-PAGE and transferred onto a PVDF membrane. Nonspecific binding was blocked by 10% dry non-fat milk in Tris-buffered saline for 1 h at RT and incubated with primary antibodies, anti-PCK1 1:1,000 (rabbit polyclonal, Genway Biotech Inc, San Diego, CA); anti-peroxiredoxin, 1:2,000 (rabbit polyclonal, Abcam, Cambridge, UK); anti-UGP2, 1:500 (mouse monoclonal, Abnova Corporation, Taipei, Taiwan); anti-FBP1, 1:1,000 (mouse polyclonal, Abnova Corporation); anti-CPS1, 1:200 (goat polyclonal); anti-GRP 78, 1:200 (rabbit polyclonal); anti-PGK1, 1:200 (goat polyclonal, all three Santa Cruz Biotechnology Inc., Heidelberg, Germany) diluted with 0.5% Tween and 0.5% BSA in Tris-buffered saline. Membranes were washed 3x with TBS-tween and incubated with secondary antibodies, goat anti-mouse IgG-HRP, 1:5,000 (Millipore, CA, USA); goat anti-rabbit IgG-HRP, 1:5,000 (Millipore); bovine anti goat IgG-HRP, 1:5,000 (Santa Cruz Biotechnology Inc.) diluted with 0.5% Tween and 0.5% BSA in Tris-buffered saline. Protein visualization was carried out using ECL™ Western blot detection reagent (GE Healthcare, Munich, Germany). To confirm equal loading, mouse monoclonal β -Actin, 1:1,000 (Sigma Immunochemicals, St. Louis, MO, USA) was used. Reprobing of all membranes was conducted using Western blot recycling kit (Alpha Diagnostic, TX, USA) according to the manufacturer's instructions.

SPANDIDOS *MS analysis and bioinformatics.* After manual gel el pieces underwent in-gel digestion (9) which was adapted for use on a Microlab Star digestion robot (Bonaduz, Switzerland) (10). Samples were reduced, alkylated, and digested using trypsin (Sigma Aldrich, Saint Louis, MO). The extracts were dried and stored at -20°C until analysis. MALDI-TOF-MS and MALDI TOF/TOF MS/MS experiments were performed on a 4800 MALDI TOF/TOFTM Analyzer (Applied Biosystems, Foster City, CA). Samples were dissolved in $5\ \mu\text{l}$ of water/acetonitrile/TFA (29.5/70/0.5, v/v/v). α -cyano-4-hydroxycinnamic acid (3 mg/ml) (Bruker Daltonics Inc., Manning Park Billerica, MA) in water/acetonitrile/TFA (29.5/70/0.5, v/v/v) was used as matrix. Analyte and matrix were spotted consecutively in a 1:1 ratio and dried under ambient conditions. The dried sample was washed with ice-cold 5% formic acid to reduce salt contamination prior to analysis. Spectra were externally calibrated with a Sequazyme Peptide Mass Standards kit (Applied Biosystems). All spectra were processed using 4,000 peak explorer (noise filtering with correlation factor, 0.7; and advanced baseline correction with peak width, 32; flexibility, 0.5; degree, 0.1). Combined peaklists of each analysed sample were generated by peaks to mascot (Applied Biosystems) using deisotoped peaks with a signal to noise ratio of at least 15 for MALDI-TOF and 4 for MALDI-TOF/TOF data. Proteins were identified by Mascot (www.matrixscience.com, Matrix Science, Boston, MA) (peptide mass tolerance, 60 ppm; fragment mass tolerance, ± 0.5 Da; maximum missed cleavages, 1) using the online NCBI database (4872416 sequences; 1684850502 residues). Proteins with a score ≥ 79 were considered significant ($p < 0.05$).

Results

Patient selection and demographic data. The patient samples for hepatocyte harvesting and isolation were selected according to their clinical history and intraoperative findings. Hepatocyte vitality was measured by trypan blue exclusion (78%, $\pm 3.2\%$). Patient 1 (female, 55 years), patient 2 (female, 66 years) and patient 3 (female, 52 years) were resected for colorectal liver metastasis. Patient 4 (male, 64 years) underwent liver resection for liver cell adenoma.

LDH-release and oxygen levels. In order to analyze the proportion of cells with membrane damage and leakage as a consequence of cell death, an LDH cytotoxicity assay was performed (8). To ensure a valid control for the HR group it was relevant to exclude differing proportions of damaged cells in the two culture groups in order to rule out artifacts from proteome changes which are not due to regulation of living cells. The measurement of cytotoxicity 24 h after hypoxia and reoxygenation (HR) or normoxic (N) cultivation did not differ significantly between the groups (N, $21 \pm 13\%$ vs. HR, $27 \pm 15\%$, n.s.). Additionally oxygen levels under HR conditions were monitored and maintained between 13.5-15% under N_2 -atmosphere. In contrast, control oxygen values lay between 140 and 150%.

Protein abundance differences and protein identification. Using 2-DE, 401 ± 40 distinct spots in the N group and 351 ± 17 spots in the HR group were detected. A total of

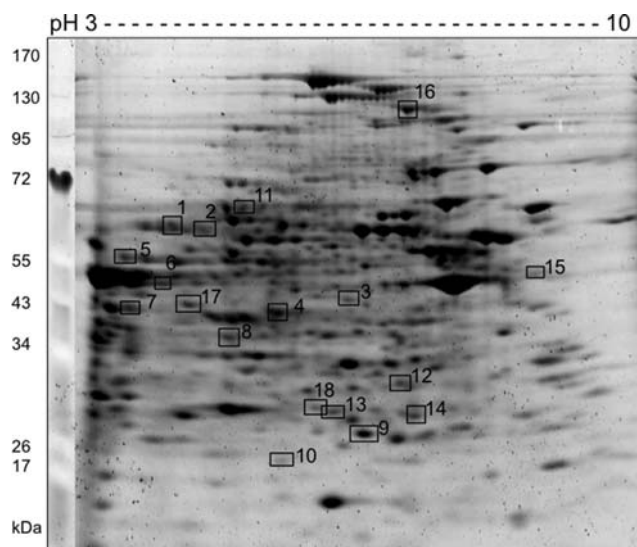


Figure 1. The 2D reference-gel (first dimension pH 3-10, second dimension 4-12% bis-tris gel) of pooled extracts from human hepatocytes originating from four patients and subsequent experiments are shown. The identified spots with significant abundance differences between the control group and after a sequence of hypoxia and reoxygenation are highlighted and numbered according to the text and Table I. Molecular weight markers are labeled on the left side of the gel.

509 spots were present in the reference gel allowing differential spot analysis of 262 spots (51%) present in all gels. Of these, a total of 106 spots (21%) displayed a >1.7 -fold intergroup difference which was significant (Mann-Whitney) in 33 spots (6.5%) and qualified them for further identification by MALDI-TOF-MS. Out of this group, 18 spots (3.5%) (Fig. 1) were successfully unequivocally identified by mass spectrometry (Table I).

The identified proteins can be classified according to their functional properties. One protein involved in glycogenesis [UTP-glucose-1-phosphate uridylyltransferase (UGP2)] was present in two different spots (#314 and #328), both displaying reduced levels in the HR group compared to control (normoxic cells).

The pathway of gluconeogenesis was represented by phosphoenolpyruvate carboxykinase (PCK) (#467) and up-regulated in HR. Fructose-1,6-bisphosphatase (FBP) (#481) was down-regulated in HR.

Three proteins involved in glycolysis were uniformly down-regulated in the HR group, phosphoglycerate kinase 1 (PGK1) (#376), fructose 1,6-bisphosphate aldolase (ALDOA) (#427), and glyceraldehyde-3-phosphate dehydrogenase (GAPDH) (#470).

A set of three peroxisomal proteins was also identified. Thiosulfat-sulfurtransferase (TST) (#562) was found to be down-regulated, while α -class glutathione S-transferase (GST) (#655) and hydroxyacid oxidase 1 (HAO1) (#680) were both up-regulated in the HR group.

Four enzymes and one additional protein were identified that are involved in cellular oxidative and stress protection. Catalase isoform 2 (CAT) (#281) and peroxiredoxin II (PRDX2) (#636) were both up-regulated while thioredoxin peroxidase (PRDX4) (#600) and peroxiredoxin III (PRDX3)

Table I. The significantly altered 2D-spots with corresponding identified proteins.

Running number of identified proteins	Spot number	Protein name	Symbol	Protein function	Mass	M-score	Fold difference
Glycogenesis							
1	314	UTP-glucose-1-phosphate uridylyl-transferase	UGP2	Catalytic activity: UTP + α -D-glucose 1-phosphate = diphosphate + UDP-glucose	57,101	222	-3.8
2	328	UDP-glucose pyrophosphorylase	UGP2	same as 314	49,005	179	-2.8
Gluconeogenesis							
3	467	Phosphoenolpyruvate carboxykinase	PCK	Catalytic activity: GTP + oxaloacetate = GDP + phosphoenolpyruvate + CO ₂ (reversible rate-controlling step of gluconeogenesis)	71,447	88	+3.9
4	481	Fructose-1,6-bisphosphatase	FBP	Rate limiting enzyme in gluconeogenesis: Catalytic activity: D-fructose 1,6-bisphosphate + H ₂ O = D-fructose 6-phosphate = phosphate	37,190	117	-10.4
Glycolysis							
5	376	Phosphoglycerate kinase 1	PGK1	Catalytic activity: ATP + 3-phospho-D-glycerate = ADP + 3-phospho-D-glyceroyl phosphate	41,773	140	-3.0
6	427	Fructose 1,6-bisphosphate aldolase	ALDOA	Catalytic activity: D-fructose 1,6-bisphosphate = glyceraldehyde 3-phosphate + D-glyceraldehyde	39,830	132	-5.0
7	470	Glyceraldehyde 3-phosphate dehydrogenase	GAPDH	Catalytic activity: D-glyceraldehyde 3-phosphate + phosphate + NAD ⁺ = 3-phospho-D-glyceroyl phosphate + NADH	36,202	120	-2.6
Peroxisomal proteins							
8	526	Thiosulfat-sulfurtransferase	TST	Converts cyanide (CN ⁻) to thiocyanate (SCN ⁻) Catalytic activity: Thiosulfate + cyanide \rightleftharpoons sulfite + thiocyanate)	33,636	132	-2.9
9	655	α -class glutathione S-transferase	GST	Catalytic activity: RX + glutathione \rightleftharpoons HX + R-S-glutathione (conjugation of reduced glutathione via the sulfhydryl group to electrophilic centres on potentially toxic substrates)	19,624	166	+1.7
10	680	Hydroxyacid oxidase 1	HAO1	2-hydroxyacid oxidase most active on glycolate, also active on 2-hydroxy fatty acids, Catalytic activity: (S)-2-hydroxy acid + O ₂ = 2-oxo acid + H ₂ O ₂	27,405	118	+3.6
Oxidative and cellular stress protection							
11	281	Catalase isoform 2	CAT	Catalase-peroxidase: 2 H ₂ O ₂ = O ₂ + 2 H ₂ O; donor + H ₂ O ₂ = oxidized donor + 2 H ₂ O	60,133	244	+2.2

Running number of identified proteins	Spot number	Protein name	Symbol	Protein function	Mass	M-score	Fold difference
12	600	Thioredoxin peroxidase	PRDX4	Ribonucleotide reduction: thioredoxin is oxidized from a dithiol to a disulfide, Catalytic activity: $2 R'-SH + ROOH = R'-S-S-R' + H_2O + ROH$	30,749	114	-2.1
13	630	Peroxiredoxin III	PRDX3	Catalytic activity: $2 R'-SH + ROOH \rightleftharpoons R'-S-S-R' + H_2O + ROH$	11,158	291	-2.1
14	636	Peroxiredoxin II	PRDX2	Catalytic activity: $2 R'-SH + ROOH = R'-S-S-R' + H_2O + ROH$	16,165	149	+2.6
15	430	Heat shock 70 kDa protein 5 (HSP70)	HSPA5	Chaperone, cellular stress response protein: protein folding, -assembly, -degradation	51,197	172	+2.1
Other proteins							
16	140	Carbamoyl phosphate synthetase I	CPS1	Urea cycle, arginine synthesis, Catalytic activity: $2 ATP + NH_3 + CO_2 + H_2O = 2 ADP + phosphate + carbamoyl phosphate$	165,975	371	+3.2
17	466	Annexin A2	ANXA2	Phospholipid binding protein	38,808	326	-2.7
18	624	Mitochondrial F1-ATP synthase, α subunit 1	ATP5A1	ATP generation	55,313	306	+1.9

Spot number, assigned number in 2D experiment; mass, molecular protein mass (Dalton); M-score, Mowse score (>79 , $p<0.05$); fold difference, fold densitometric abundance difference of spots from hypoxia vs. control samples.

(#630) were down-regulated in the HR group. Heat shock 70 kDa protein 5 (HSPA5) (#430) was up-regulated in the HR group.

The mitochondrial F1-ATP synthase, α subunit 1 (ATP5A1) (#624), which is involved in cellular energy metabolism, was found to be up-regulated after HR. Carbamoyl phosphate synthetase I (CPS1) (#140), a member of the urea cycle, was up-regulated in the HR group, while annexin A2 (ANXA2) (#466) was down-regulated after HR treatment.

To confirm the observed 2-DE changes of the identified proteins, Western blot analysis was done with a selection of commercially available antibodies for each HR experiment separately. Due to limited antibody availability only seven of the identified proteins could be analyzed with this immunological assay. UGP2, PCK, PGK1 and PRDX2 showed similar changes in their levels as was seen in the 2-DE experiments (Fig. 2, right panel). In contrast FBP1, CPSI, and HSP70 did not display relevant changes in the Western blot (data not shown).

Discussion

Hypoxia followed by reoxygenation is a pathophysiological stimulus under various clinical conditions. The degree of the adaptive responses depends on the duration of hypoxia. Short-term reduction of O_2 supply is followed by the

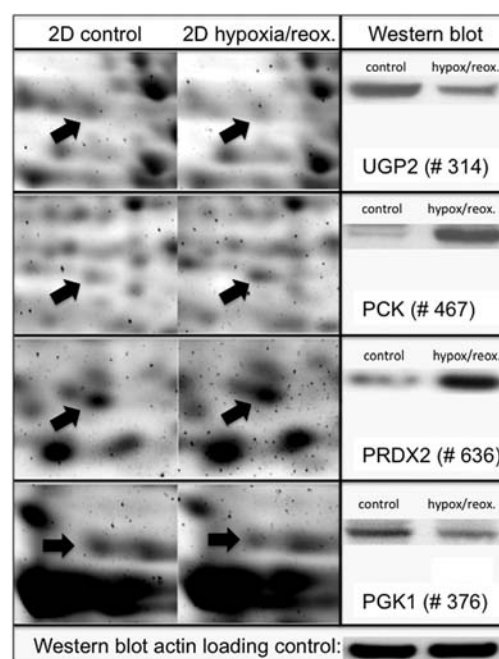


Figure 2. 2D page differences (left panels) and Western blot analysis (right panels) of pooled hepatocyte lysates under control conditions vs. hypoxia and reoxygenation for four different spots and the corresponding proteins (UGP2, PCK, PGK1, PRDX2) are depicted. Results displayed are representative for the experiments performed. Western blot for actin served as loading control.

modification of existing proteins through phosphorylation or other post-translational changes (11). When low O₂ concentration is sustained longer adaptive alterations of gene expression take place and finally chronic hypoxia results in cell death when the adaptive mechanisms are exhausted (12). Short-term hypoxia can prime cells or organs to increase their tolerance to hypoxia (13,14) for example through down-regulation of energy demanding pathways to reduce ATP requirements (15-17). Another compensatory factor is the up-regulation of protective components against reactive oxygen species generated during reoxygenation.

Since hypoxia represents a major challenge for cells, subsequent changes of gene expression, protein degradation, and other post-translational modifications should result in alteration of the proteome (18). To elucidate the global protective responses to HR in human primary hepatocytes we submitted their cultures to a sequence of hypoxia and reoxygenation. In contrast to immortalized cell lines the use of human primary hepatocytes in our analysis allows to imitate more accurately physiologic processes present *in vivo*. Proteome analysis of immortalized murine hepatoma cells revealed substantial differences to their primary counterparts (19). Following hypoxia the cellular proteome was analyzed after 24 h of reoxygenation in a steady state of oxidative cellular metabolism. These steady state conditions support the detection of prolonged proteome alterations possibly relevant for long term hepatocyte function without short-term artifacts due to cell death.

Cellular integrity and membrane damage was not significantly altered through our experimental set up as monitored by LDH release. The hepatocytes were capable of sustaining 6 h of hypoxia with O₂-values ~15 mmHg and reoxygenation without increase in LDH release. The critical level of 5 mmHg O₂ which would completely inhibit mitochondrial respiration (20,21) was always exceeded.

In this study proteome changes in three major functional protein groups, namely glucose metabolism, oxidative and cell stress protection as well as peroxisomal function were identified after the sequence of HR in human hepatocyte cultures.

Glucose metabolism. Our results illustrate that glucose metabolism remains affected even 24 h after HR. For example abundance of UGP2, involved in glycogenesis, was below control even 24 h after reoxygenation. This suggests that the cells still had not been able to regain their original energy status. UGP2 has also been shown to indirectly reduce the rate of glucuronidation under hypoxia by limiting the required substrates UTP and glucose 1-phosphate (22). The impairment of glucuronidation after LTX(23) might therefore partly be due to a prolonged down-regulation of UGP2.

The key enzyme of gluconeogenesis, FBP, was also identified. Liver net gluconeogenic flux is terminated during anoxia (24) and increasing AMP levels under anoxia act as an inhibitor of FBP (25). Although the 2-DE results indicated down-regulation of FBP, the Western blotting results showed no changes of FBP after HR. It is likely that regulation of FBP is not only influenced by changes of AMP levels but also involves post-translational changes causing a partial shift of the FBP spot in the 2D gels.

Glycolysis involves the identified enzymes PGK1, ALDOA, and GAPDH, which have all been linked to hypoxia dependent

adaptation. PGK1 triggers HIF-1 α -dependent gene transcription in response to hypoxia (26,27). ALDOA is up-regulated under hypoxia in astrocytes (28). GAPDH can form a complex with a ubiquitin ligase which initiates degradation of nuclear proteins during apoptosis (29). GAPDH also participates in the formation of the OCA-S transcriptional coactivator complex connecting the cellular metabolic state to gene transcription (30).

The reduced levels of the described glycolytic enzymes in our experiments after HR might reflect a compensatory metabolic state, which suppresses glycolysis under normoxic conditions after hypoxia to enhance restoration of glycogen and glucose levels.

Peroxisomal detoxification. The levels of three peroxisomal enzymes, TST, GST and HAO1, were altered due to HR. TST, a sulphur transferase, has a higher turnover rate under hypoxia and detoxifies cyanide (31). Our cells had a reduced abundance of TST after HR. GST, increased after HR, catalyses the addition of glutathione to different electrophiles resulting in protection against toxic substrates (32). An increase of GST activity under hypoxia was found in endothelial cells, medaka brain tissue (33), and in the frog *Rana pipiens* (34). Increase of GST activity is also required for hypoxia-dependent changes of the intracellular redox potential (35). Taken together, these findings stand in line with our observation of an anoxia-responsive regulation of GST.

HAO1, a liver specific oxidase (36), was also up-regulated after HR. Oxidase activity generates the reactive oxygen species hydrogen peroxide. Notably, in the context of HR peroxisomal oxidases are only minor contributors to the reactive oxygen species pool in hepatocytes especially in the presence of catalase activity (37).

Oxidative and cell stress protection. Four peroxiredoxins were differentially regulated after HR, CAT and PRDX2 (up-regulated), PRDX3 and -4 (down-regulated). Peroxidases (PRX) have a conserved Cys residue that undergoes oxidation and thiol-dependent reduction (38) during the removal of peroxides (39). Oxidation of PRX in the context of LTX is influenced by warm ischemia time (40) and PRX1 and -2 are induced during LTX resulting in protection against oxidant damage (41). Therefore, PRX induction might be an approach to protect transplant organs against IRI. This has already been shown in a murine IRI gene transfer model (42).

HSP70 has already been implicated in the cellular response to HR (43). Induction of HSP70 attenuated IRI in rat hearts (44) and during LTX (45). HSP70 expression does not occur during the stress period itself but during recovery after the noxae (18). This is supported by our finding of an HSP70 increase after reoxygenation. Again post-translational changes might explain the lack of Western blotting confirmation for the 2-DE changes in HSP70 abundance as phosphorylation of chaperones can result in a shift on the 2-DE page (46).

Proteins from other areas of cellular metabolism. Four proteins were identified originating from other metabolic contexts. CPS1 (urea cycle) influences the substrate L-arginine (47,48). L-arginine, the major source for NO, mainly originates from liver synthesis (49,50), and protects against IRI (51,52). It is intriguing to hypothesize that CPS1 up-regulation, as seen in



SPANDIDOS[®], contributes to protection from oxidative damage PUBLICATIONS

ANXA2, also up-regulated after HR, is a phospholipid- and membrane binding protein. ANXA2 has been shown to protect neurons and glial cells against hypoxia injuries (53). Therefore, the observed ANXA2 up-regulation confirms previous findings and supports its role during hypoxic stress.

ATP5A1, a mitochondrial ATP-synthase up-regulated after HR, hydrolyzes ATP to counteract the collapse of the proton motive force under hypoxic conditions. Thus ATP consumption by ATP-synthase must be limited under anoxic conditions by inhibition of the enzyme (54,55). It was proposed that mitochondria are regulated at the level of the ATP-synthase *in vivo* (56). This regulation involves gene expression changes as shown after HR in astrocytes. Interestingly, hypoxia alone did not induce ATP-synthase gene expression but it occurred after reoxygenation (57).

The proteomic analysis of hepatocytes submitted to sequential hypoxia and reoxygenation revealed three major metabolic areas to be affected in response to the stimulus. Among these were glucose and glycogen metabolism (six proteins), the process of peroxisomal detoxification (three proteins) and mechanisms of oxidative and cellular stress protection (five proteins). Many of the proteins identified have already been implicated in the context of cellular adaptation mechanisms in response to HR. It appears that phylogenetically old protective mechanisms play a role in stabilizing hepatic cellular functions. Further studies are needed to elucidate the relevance of the observed enzyme and protein changes in the clinical setting. Some proteins might have diagnostic potential in the evaluation of liver graft quality or could serve to monitor therapeutic interventions such as glucose supply to potential organ donors to optimise the energy status of the organs to be harvested (58).

References

- Lau AT, He QY and Chiu JF: Proteomic technology and its biomedical applications. *Sheng Wu Hua Xue Yu Sheng Wu Wu Li Xue Bao (Shanghai)* 35: 965-975, 2003.
- Mann M, Hendrickson RC and Pandey A: Analysis of proteins and proteomes by mass spectrometry. *Annu Rev Biochem* 70: 437-473, 2001.
- Strey CW, Winters MS, Markiewski MM and Lambris JD: Partial hepatectomy induced liver proteome changes in mice. *Proteomics* 5: 318-325, 2005.
- Hanash SM, Madoz-Gurpide J and Misek DE: Identification of novel targets for cancer therapy using expression proteomics. *Leukemia* 16: 478-485, 2002.
- Jungblut PR, Zimny-Arndt U, Zeindl-Eberhart E, *et al*: Proteomics in human disease: cancer, heart and infectious diseases. *Electrophoresis* 20: 2100-2110, 1999.
- Strey CW, Spellman D, Stieber A, Gonatas JO, Wang X, Lambris JD and Gonatas NK: Dysregulation of stathmin, a microtubule-destabilizing protein, and up-regulation of Hsp25, Hsp27, and the antioxidant peroxiredoxin 6 in a mouse model of familial amyotrophic lateral sclerosis. *Am J Pathol* 165: 1701-1718, 2004.
- Leckel K, Strey C, Bechstein WO, *et al*: Autocrine stimulation of human hepatocytes triggers late DNA synthesis and stabilizes long-term differentiation *in vitro*. *Int J Mol Med* 21: 611-620, 2008.
- Mukhin AG, Ivanova SA, Allen JW and Faden AI: Mechanical injury to neuronal/glial cultures in microplates: role of NMDA receptors and pH in secondary neuronal cell death. *J Neurosci Res* 51: 748-758, 1998.
- Shevchenko A, Wilm M, Vorm O and Mann M: Mass spectrometric sequencing of proteins silver-stained polyacrylamide gels. *Anal Chem* 68: 850-858, 1996.
- Corvey C, Koetter P, Beckhaus T, *et al*: Carbon Source-dependent assembly of the Snf1p kinase complex in *Candida albicans*. *J Biol Chem* 280: 25323-25330, 2005.
- Chandel NS, Budinger GR and Schumacker PT: Molecular oxygen modulates cytochrome c oxidase function. *J Biol Chem* 271: 18672-18677, 1996.
- Schumacker PT, Chandel N and Agusti AG: Oxygen conformance of cellular respiration in hepatocytes. *Am J Physiol* 265: L395-L402, 1993.
- Amador A, Grande L, Marti J, *et al*: Ischemic pre-conditioning in deceased donor liver transplantation: a prospective randomized clinical trial. *Am J Transplant* 7: 2180-2189, 2007.
- Massip-Salcedo M, Rosello-Catafau J, Prieto J, Avila MA and Peralta C: The response of the hepatocyte to ischemia. *Liver Int* 27: 6-16, 2007.
- Hochachka PW and Lutz PL: Mechanism, origin, and evolution of anoxia tolerance in animals. *Comp Biochem Physiol B Biochem Mol Biol* 130: 435-459, 2001.
- Subramanian RM, Chandel N, Budinger GR and Schumacker PT: Hypoxic conformance of metabolism in primary rat hepatocytes: a model of hepatic hibernation. *Hepatology* 45: 455-464, 2007.
- Jungermann K and Kietzmann T: Oxygen: modulator of metabolic zonation and disease of the liver. *Hepatology* 31: 255-260, 2000.
- Storey KB: Metabolic adaptations supporting anoxia tolerance in reptiles: recent advances. *Comp Biochem Physiol B Biochem Mol Biol* 113: 23-35, 1996.
- Pan C, Kumar C, Bohl S, Klingmueller U and Mann M: Comparative proteomic phenotyping of cell lines and primary cells to assess preservation of cell type-specific functions. *Mol Cell Proteomics* 8: 443-450, 2009.
- Wilson DF, Rumsey WL, Green TJ and Vanderkooi JM: The oxygen dependence of mitochondrial oxidative phosphorylation measured by a new optical method for measuring oxygen concentration. *J Biol Chem* 263: 2712-2718, 1988.
- Longmuir IS: Respiration rate of rat-liver cells at low oxygen concentrations. *Biochem J* 65: 378-382, 1957.
- Aw TY and Jones DP: Control of glucuronidation during hypoxia. Limitation by UDP-glucose pyrophosphorylase. *Biochem J* 219: 707-712, 1984.
- Park JM, Lin YS, Calamia JC, *et al*: Transiently altered acetaminophen metabolism after liver transplantation. *Clin Pharmacol Ther* 73: 545-553, 2003.
- Clark MG, Bloxham DP, Holland PC and Lardy HA: Estimation of the fructose 1,6-diphosphatase-phosphofructokinase substrate cycle and its relationship to gluconeogenesis in rat liver *in vivo*. *J Biol Chem* 249: 279-290, 1974.
- Horecker BL and Pontremoli S: The Enzymes. Vol IV. Boyer PD (ed). Academic Press, New York, p611, 1971.
- Firth JD, Ebert BL, Pugh CW and Ratcliffe PJ: Oxygen-regulated control elements in the phosphoglycerate kinase 1 and lactate dehydrogenase A genes: similarities with the erythropoietin 3' enhancer. *Proc Natl Acad Sci USA* 91: 6496-6500, 1994.
- Luo F, Liu X, Yan N, *et al*: Hypoxia-inducible transcription factor-1 α promotes hypoxia-induced A549 apoptosis via a mechanism that involves the glycolysis pathway. *BMC Cancer* 6: 26, 2006.
- Niitsu Y, Hori O, Yamaguchi A, *et al*: Exposure of cultured primary rat astrocytes to hypoxia results in intracellular glucose depletion and induction of glycolytic enzymes. *Brain Res Mol Brain Res* 74: 26-34, 1999.
- Hara MR, Agrawal N, Kim SF, *et al*: S-nitrosylated GAPDH initiates apoptotic cell death by nuclear translocation following Siah1 binding. *Nat Cell Biol* 7: 665-674, 2005.
- Zheng L, Roeder RG and Luo Y: S phase activation of the histone H2B promoter by OCA-S, a coactivator complex that contains GAPDH as a key component. *Cell* 114: 255-266, 2003.
- Westley J: Enzymatic Basis of Detoxication. Vol 2. Jacoby WB (ed). Academic Press, New York, pp245-262, 1980.
- Willmore WG and Storey KB: Purification and properties of the glutathione S-transferases from the anoxia-tolerant turtle, *Trachemys scripta elegans*. *FEBS J* 272: 3602-3614, 2005.
- Oehlers LP, Perez AN and Walter RB: Detection of hypoxia-related proteins in medaka (*Oryzias latipes*) brain tissue by difference gel electrophoresis and de novo sequencing of 4-sulfophenyl isothiocyanate-derivatized peptides by matrix-assisted laser desorption/ionization time-of-flight mass spectrometry. *Comp Biochem Physiol C Toxicol Pharmacol* 145: 120-133, 2007.

34. Hermes-Lima M and Storey KB: Role of antioxidant defenses in the tolerance of severe dehydration by anurans. The case of the leopard frog *Rana pipiens*. *Mol Cell Biochem* 189: 79-89, 1998.
35. Millar TM, Phan V and Tibbles LA: ROS generation in endothelial hypoxia and reoxygenation stimulates MAP kinase signaling and kinase-dependent neutrophil recruitment. *Free Radic Biol Med* 42: 1165-1177, 2007.
36. Van den Munckhof RJ: In situ heterogeneity of peroxisomal oxidase activities: an update. *Histochem J* 28: 401-429, 1996.
37. Siraki AG, Pourahmad J, Chan TS, Khan S and O'Brien PJ: Endogenous and endobiotic induced reactive oxygen species formation by isolated hepatocytes. *Free Radic Biol Med* 32: 2-10, 2002.
38. Arner ES and Holmgren A: Physiological functions of thioredoxin and thioredoxin reductase. *Eur J Biochem* 267: 6102-6109, 2000.
39. Blokhina O, Virolainen E and Fagerstedt KV: Antioxidants, oxidative damage and oxygen deprivation stress: a review. *Ann Bot* 91: 179-194, 2003.
40. Avellini C, Baccarani U, Trevisan G, *et al*: Redox proteomics and immunohistology to study molecular events during ischemia-reperfusion in human liver. *Transplant Proc* 39: 1755-1760, 2007.
41. Shau H, Merino A, Chen L, Shih CC and Colquhoun SD: Induction of peroxiredoxins in transplanted livers and demonstration of their in vitro cytoprotection activity. *Antioxid Redox Signal* 2: 347-354, 2000.
42. He SQ, Zhang YH, Venugopal SK, *et al*: Delivery of anti-oxidative enzyme genes protects against ischemia/reperfusion-induced liver injury in mice. *Liver Transpl* 12: 1869-1879, 2006.
43. Gething MJ and Sambrook J: Protein folding in the cell. *Nature* 355: 33-45, 1992.
44. Hutter MM, Sievers RE, Barbosa V and Wolfe CL: Heat-shock protein induction in rat hearts. A direct correlation between the amount of heat-shock protein induced and the degree of myocardial protection. *Circulation* 89: 355-360, 1994.
45. Flohe S, Speidel N, Flach R, Lange R, Erhard J and Schade FU: Expression of HSP 70 as a potential prognostic marker for acute rejection in human liver transplantation. *Transpl Int* 11: 89-94, 1998.
46. Krishna SB, Alfonso LF, Thekkumkara TJ, Abbruscato TJ and Bhat GJ: Angiotensin II induces phosphorylation of glucose-regulated protein-75 in WB rat liver cells. *Arch Biochem Biophys* 457: 16-28, 2007.
47. Summar ML, Hall L, Christman B, *et al*: Environmentally determined genetic expression: clinical correlates with molecular variants of carbamyl phosphate synthetase I. *Mol Genet Metab* 81: S12-S19, 2004.
48. Pearson DL, Dawling S, Walsh WF, *et al*: Neonatal pulmonary hypertension - urea-cycle intermediates, nitric oxide production, and carbamoylphosphate synthetase function. *N Engl J Med* 344: 1832-1838, 2001.
49. Featherston WR, Rogers QR and Freedland RA: Relative importance of kidney and liver in synthesis of arginine by the rat. *Am J Physiol* 224: 127-129, 1973.
50. Darmaun D, Welch S, Rini A, Sager BK, Altomare A and Haymond MW: Phenylbutyrate-induced glutamine depletion in humans: effect on leucine metabolism. *Am J Physiol* 274: E801-E807, 1998.
51. Li SQ and Liang LJ: Protective mechanism of L-arginine against liver ischemic-reperfusion injury in rats. *Hepatobiliary Pancreat Dis Int* 2: 549-552, 2003.
52. Tuncer MC, Ozturk H, Buyukbayram H and Ozturk H: Interaction of L-arginine-methyl ester and Sonic hedgehog in liver ischemia-reperfusion injury in the rats. *World J Gastroenterol* 13: 3841-3846, 2007.
53. Han S, Zhang KH, Lu PH and Xu XM: Effects of annexins II and V on survival of neurons and astrocytes in vitro. *Acta Pharmacol Sin* 25: 602-610, 2004.
54. St Pierre J, Brand MD and Boutilier RG: Mitochondria as ATP consumers: cellular treason in anoxia. *Proc Natl Acad Sci USA* 97: 8670-8674, 2000.
55. Scholz TD and Balaban RS: Mitochondrial F1-ATPase activity of canine myocardium: effects of hypoxia and stimulation. *Am J Physiol* 266: H2396-H2403, 1994.
56. Das AM and Harris DA: Regulation of the mitochondrial ATP synthase in intact rat cardiomyocytes. *Biochem J* 266: 355-361, 1990.
57. Kasai K, Yamashita T, Yamaguchi A, *et al*: Induction of mRNAs and proteins for Na/K ATPase alpha1 and beta1 subunits following hypoxia/reoxygenation in astrocytes. *Brain Res Mol Brain Res* 110: 38-44, 2003.
58. Singer P, Cohen J and Cynober L: Effect of nutritional state of brain-dead organ donor on transplantation. *Nutrition* 17: 948-952, 2001.